LS47: A DSN Station Location Set Compatible With JPL Development Ephemeris DE108

J. Ellis
Navigation Systems Section

An updated DSN station location set, LS47, is presented which is compatible with JPL Development Ephemeris DE108. Analytic procedures for linearly correcting station spin axis and longitude estimates for an ephemeris update based on Brouwer-Clemence Set III parameters are briefly discussed. The validity of this technique is demonstrated by a comparison of a linearly corrected solution with one explicitly determined by reprocessing the data. A mission data base, including Viking 1 and 2 encounter data, is first used to obtain an updated DE96 compatible station location solution, LS46, which in turn is adjusted to form the DE 108 solution, LS47. Improved station Z-heights are estimated by using available very long baseline interferometry (VLBI) data. Spin axis differences between LS46 and LS47 are relatively insignificant; however, the ephemeris change introduces a -0.8×10^{-5} *degree rotation in the DE96 longitude ephemeris.*

I. Introduction

This article presents a set of station location estimates for navigation support for Voyager Jupiter encounter and Pioneer-Venus operations. The new solution, Location Set (LS)47, is compatible with JPL Development Ephemeris DE108 (Ref. 1), which will be used for navigation by these projects. LS47 replaces the DE96 compatible station solution set LS45 (Refs. 2 and 3) which supported Voyager and Pioneer-Venus launch and cruise operations.

Several significant changes have been made in the procedures for updating station spin axis and longitude estimates for an ephemeris change and in the mission set data base and auxiliary source data used to determine station locations. These changes include the following:

(1) Development of analytic techniques for correcting station spin radius and longitude estimates for an ephemeris change.

(2) Addition of Viking 1 and Viking 2 encounter data to the mission set data base.

(3) Treatment of geodetic survey data directly as additional observations.

(4) Use of very long baseline interferometry (VLBI) data to determine Z-heights.

A comprehensive software system and supporting data base have been designed and implemented for generating station location estimates and analytically correcting station spin radii and longitudes for an ephemeris update. The major advantage of this approach is that it eliminates the need to repeat the orbit determination process when an ephemeris is replaced. This system combined with the data base is expected to form the foundation for future station location efforts. As such, LS47 is the first set to be generated based on this new system. A brief discussion of the computational techniques is presented in this article. Details of the procedure and software implementation will be discussed in a future article.

Considerable effort has been expended in developing and validating these procedures. As a preliminary step, a DE96 compatible station location set LS46 was computed to evaluate the effect of changes in the mission set data base and the software. Solution sets for LS45 and LS46 were compared to determine the effect of the above changes. Finally, station solutions LS47 and LS46 were compared to determine the effect of the ephemeris change.

II. Computational Procedures for Station Location Determination

A. Correcting for an Ephemeris Update

DSN station locations are computed in a geocentric reference frame defined by the Earth's mean pole (axis of rotation), equator and prime meridian of 1903.0. The location of the station with respect to this frame is expressed in cylindrical coordinates r_s, λ and Z_s, where

r_s = "distance from" the axis of rotation (spin axis)

λ = longitude as measured east from the prime meridian

Z_s = height above equator plane (Z-height)

The conventional procedure for estimating the coordinates of the tracking station is based on using a data base consisting of radio metric tracking data from a set of planetary encounter missions to provide an accurate determination of the planet-relative spacecraft state. This knowledge combined with the planetary direction information inherent in the planetary ephemeris is used to determine a least squares solution for the station spin axis and longitude. Historically, updating a DSN station location set to account for an ephemeris change has required reprocessing the radio metric data for all missions in the data base. A complete refit of the radio metric data for each mission is repeated using the Double Precision Orbit Determination Program (DPODP). This requires iterating to convergence for a new trajectory which best fits the data using the new planetary ephemeris.

The useful results of each such data fit can be compactly represented in terms of a triangularized information array, referred to as the data equation; i.e.,

$$Z = Rx + \eta \tag{1}$$

where

x = the parameters to be estimated

R = the "packed" information matrix

η = the measurement error

Z = the "packed" data residuals

The conventional procedure is to statistically combine the information arrays for all missions in the data base and to estimate the spin axis and longitude from the combined information matrix.

The basic disadvantage of this approach is that it requires lengthy and costly DPODP runs to obtain each information array compatible with an updated ephemeris. A way of avoiding this is to recognize that a small ephemeris change can be expressed as a linear perturbation to the nominal data residuals. The perturbation due to the ephemeris change can in turn be *approximated* in terms of the partials of the observations with respect to the appropriate Brouwer and Clemence Set III parameters (Ref. 4) and the planetary mass, and the actual Set III and mass correction, from the "nominal" ephemeris; i.e.,

$$Z_{new} = Z + \frac{\delta Z}{\delta E}\Delta E + \frac{\delta Z}{\delta m}\Delta m \tag{2}$$

where E are the Brouwer and Clemence Set III parameters for the target body and the Earth, m is the planetary mass of the target body, and Z_{new}, Z are the data residuals.

Corrections ΔE, in turn, are approximated by transforming the differences of the cartesian positions and velocities of the target body and the Earth-Moon barycenter at the mission encounter time to Set III corrections defined at the osculating epoch of the ephemeris. Mass differences are simply determined by reading the new and nominal ephemerides files.

This technique had been suggested in a memo by H. Koble (Ref. 5); however, its accuracy had never been verified. For purposes of testing the procedure, DE96 station location estimates obtained from DPODP runs were compared with an equivalent DE84 data base which had been linearly corrected to DE96. Solutions were determined for each individual mission as well as for the combined data set. The maximum differences observed in the station spin radius and longitude estimates were 0.02 meters and 0.03×10^{-5} degrees respectively, which are significantly below our estimation accuracies of 0.6m and 2.0×10^{-5} deg.

In practice a "nominal" mission data base has been established which is based on the DE96 ephemeris and the LS43 station set. Information arrays for all missions have been standardized to DE96. This data base will form the data set for the current and future station location efforts and will be expanded to include new data when available.

B. Geodetic Survey Information

A second major difference in the computational procedures is the manner in which geodetic survey information is treated.

The final station location estimates are determined by adjoining the geodetic survey information (Ref. 6) to the combined information array for the individual missions. For the LS45 determination the relative survey information was treated as an a priori covariance constraint (Ref. 5). For stations related by survey information, the correlation coefficient of the spin radius and longitude a priori covariance were computed to reflect the survey accuracy of 0.3m and 0.3×10^{-5} deg.

The above procedure suffers from the deficiency that it assumes the a priori values of the station location estimates satisfy the relative coordinate difference specified by the geodetic survey measurements. For LS46 and LS47, geodetic survey measurements were included directly as additional observations, with accuracies of a 0.3 m for spin radius and 0.3×10^{-5} deg for longitude. This approach has the further advantage that it can be expanded to include other relative data types, such as VLBI data.

C. Station Z-height Determination

Since station Z-heights cannot be determined from conventional radio metric data, it is necessary to rely on other data sources to compute Z-heights. The LS45 Z-heights were computed by combining the results of geodetic surveys (Ref. 6) made at the various sites with the geocentric-geodetic differences obtained from optical and laser data (Ref. 7). The availability of preliminary VLBI results (Ref. 8) provides us with an additional source for determining intercontinental relative Z-heights. The strategy adopted for computing Z-heights for LS47 consisted of the following:

(1) The absolute Z-height for DSS 14 was computed by correcting the geodetic survey value for the datum correction.

(2) The Z-heights of DSS 43 and DSS 63 were then determined from the VLBI intercontinental baseline observations for the polar component (i.e., relative 14-63, 14-43 Z-height differences).

(3) The relative geodetic survey data was then used to compute Z-heights for the remaining stations (DSS 11, 12, 13, 42, 44, 61, 62) within each complex.

(4) Since no VLBI data was available for DSS 41 and DSS 51, the LS45 Z-height values were retained for these stations.

Tables 1 and 2 summarize the geodetic and VLBI data that were used. This procedure is equivalent to replacing the laser and optically determined Z-heights offsets, which have a one-sigma accuracy of 5 meters, with equivalent VLBI information which has a reported accuracy of 1.2 meters. The maximum difference between the LS47 and LS45 Z-heights is 4.7 m, which is consistent with the quoted accuracy of the LS45 set of 15m.

III. Location Set 47

A. Mission Data Base

LS47 spin radius and longitude estimates are based on a mission data set which includes the original LS45 data base supplemented with the Viking 1 and Viking 2 encounter data (Ref. 9). The complete data set is summarized in Table 3. The LS45 data base includes the planetary encounter data arcs for Mariners 4, 5, 6, 9, 10-Venus and 10-Mercury (first encounter) as well as zero declination data arcs for Mariner 5 pre- and post-encounter. Each mission data set uses the best BIH timing and polar motion data and calibrations for troposphere, ionosphere and space plasma. Only radio metric data calibrated for charged particle effects are included in the final Viking data set.

For consistency, the parameter solution sets for the Mariner 10 encounters were modified relative to those used for LS45 analysis. The planet mass and oblateness were eliminated from the estimated parameter set. For the Venus encounter arc a 9-parameter solar pressure model was added, so that the complete set of estimated parameters included the spacecraft state, solar pressure and the station locations. The final solution set for the Mariner 10 Mercury encounter includes the spacecraft state, solar pressure, range bias and station locations. Parameter sets for the remaining missions were identical to the sets which produced the LS45 results (Refs. 2 and 3).

B. DE96 Compatible Solution, LS46

As a preliminary step in deriving LS47, a DE96 compatible solution set, designated LS46, was initially generated to evaluate the effects of the various data base changes on the station solutions. LS46 represents an "updated" LS45 solution which includes the additional Viking encounter data, the effect of parameter set modifications, changes in the computational procedure and the application of VLBI data. Both solutions are documented in Tables 4 and 5, with differences and the effect of the Viking data summarized in Table 6. The maximum spin radius and longitude differences between LS45 and LS46 are 0.1 m and 0.33×10^{-5} deg, respectively. Use of the VLBI data introduces a Z-height change of -4.7 m for DSS 42, 43 and 44, and a change of +4.1 m for DSS 61, 62 and 63. In summarizing, it appears that the addition of the Viking data as well as the other changes has a small effect on the combined spin axis and longitude solution. The new results are within the 0.6 m spin axis and 2.0×10^{-5} deg longitude accuracies quoted for LS45 (Refs. 2 and 5).

C. DE108 Compatible Solution, LS47

The LS47 solution, presented in Table 7, is the result of linearly correcting the LS46 spin axis and longitudes to account for differences in the DE108 and 96 ephemerides. The resulting differences between the LS47 and LS46 solutions are listed in Table 8. While spin axis differences are statistically insignificant, DE108 longitudes are rotated approximately 0.8×10^{-5} deg west relative to the DE96 values.

The change in station location due to an ephemeris update can be approximated from the differences in the geocentric right ascensions and declinations of the target body at encounter time. The relationship is given by

$$\Delta r_s = r_s \Delta\delta \tan\delta$$

$$\Delta\lambda = \Delta\alpha$$

where

r_s = the station spin radius

λ = the station longitude

δ = the target body declination

α = the target body right ascension

Figure 1 plots the differences in DE108 and DE96 right ascensions at the encounter times. There is a clear secular trend of -0.15×10^{-5} deg/year for the right ascension differences between DE108 and DE96, which translates into longitude corrections that range from 0.27×10^{-5} deg for Mariner 4 to -1.08×10^{-5} deg for Viking B. The -0.8×10^{-5} change for the combined set represents a weighted average of the DE108-DE96 right ascension changes. The maximum predicted spin axis change is approximately 0.12 m.

The effect of the secular trend in right ascension on the LS47 solution can be observed by plotting the difference between the individual data arc solutions for each mission and the combined solutions. These differences are plotted for LS46 and LS47 in Figs. 2 through 5. Each difference is plotted along with its formal standard deviation as a vertical bar, with the length of the bar determined by the formal standard deviation of each solution and the expected difference represented by a horizontal line. A comparison of these plots for LS46 and LS47 reveals that the spin radius differences are approximately the same, whereas the longitude differences appear to be rotated. The LS47 longitude scatter is the result of a rotation of the abscissa of the LS46 scatter about a center approximated by the Mariner 10 encounter time, with the resulting slope of 0.15×10^{-5} deg. This result is predictable from a weighted least squares analysis of the effect of a rotation of the longitudes from DE96 to DE108.

An examination of the individual mission error plots for LS46 and LS47, as well as similar figures for LS44 (Refs. 2 and 9), reveals several disturbing anomalies which have not been satisfactorily explained. Basically, the plots for LS46 and LS44 are similar, as expected. The inconsistencies in the individual solutions for the "earlier" missions, Mariners 4, 5, and 6, may largely be due to the procedures for reconstructing ad hoc calibrations. For the more recent missions, Mariner 10 Mercury solutions for DSS 12 and 42 appear to be inconsistent, while the Viking solutions exhibit a disturbing inconsistency in the spin axis solution for DSS 11.

D. DSS 12 Conversion to 34-Meter Antenna

DSS 12 has recently been converted from a 26- to a 34-m antenna. This conversion entailed a 10-ft vertical displacement of the antenna with respect to the local gravity vector. The tolerance of this vertical displacement is 1/10,000 of a foot. Since an updated survey was not available, spin axis and Z-height coordinates for DSS 12 were computed by transforming the 10-ft vertical displacement to geodetic spin axis and Z-height components. Table 7 lists the coordinates for DSS 12 before and after the conversion.

E. Station Location Estimates for DSS 13 and 14

Radio metric data was not available in the current mission set data base for DSS 13 and 44. As a result, the coordinates for the nonparticipating stations were based strictly on relative geodetic survey information. DSS 13 coordinates were computed from relative survey differences between DSS 12 and 13. Relative survey differences between DSS 42 and 44 were used to compute the DSS 44 locations.

IV. Summary and Future Directions

An analytic procedure has been developed for linearly correcting station location estimates for an ephemeris update. The validity of the procedure has been demonstrated and the technique has been applied to computing a station location set LS47 compatible with ephemeris DE108. Spin axis differences between LS45, LS46, and LS47 are relatively insignificant. However, the ephemeris change introduces a -0.8×10^{-5} deg rotation in the DE96 longitude estimates.

Based on a series of parametric studies (Refs. 2 and 5) it was concluded that the maximum 1-sigma errors for LS45 spin axis and longitudes were bounded by 0.6 m and 2.0×10^{-5} deg, respectively, relative to DE96. These error bounds were applicable to stations for which radio metric data was available. The same level of confidence can be established for the LS46 solution, which agrees with LS45 to within 0.1 m in spin radius and 0.33×10^{-5} deg in longitude. Since the same data base, calibrations and basic procedures were used for LS46 and

LS47, the accuracy of the LS47 set can be expected to be comparable *relative to DE108.*

Several areas are currently being explored in an attempt to improve the LS47 station estimates and to confirm the quoted accuracies. These include the following:

(1) Evaluation of the feasibility of incorporating Viking orbiter and lander data.

(2) Utilization of VLBI data for improving relative spin, radius and longitude estimates.

(3) Evaluation of precession effects on longitude solutions.

(4) Evaluation of updated survey information.

(5) Application of filtering strategies which weight results from recent missions more heavily than results from the earlier missions.

Any adjustments to the LS47 station set based on the above efforts are expected to be available for the final Voyager encounter lockfile.

Acknowledgment

The author wishes to acknowledge the assistance of R. Henderson, G. Pease and J. Gliniak for their contributions in developing and implementing the computer software and performing the computer runs. C. Thornton, H. Koble and N. Mottinger were responsible for the basic computer software, for updating and combining information arrays, and for assistance in analyzing the results.

References

1. Standish, E. M., "DE108 Announcement," IOM 315.5-132, Jet Propulsion Laboratory, Pasadena, Calif., Oct. 6, 1978 (an internal document).

2. Koble, H. M., "LS45 A Station Location Set Compatible with DE96," IOM 314.5-87, Jet Propulsion Laboratory, Pasadena, Calif., May 20, 1977 (an internal document).

3. Koble, H. M., "Recommended Update to DSS 44 Location Estimates," IOM 314.5-100, Jet Propulsion Laboratory, Pasadena, Calif., Oct. 27, 1977 (an internal document).

4. Brouwer, D. and Clemence, G. M., *Methods of Celestial Mechanics*, Academic Press, 1961.

5. Koble, H. M., "LS44 - An Improved Deep Space Network Station Location Set for Viking Navigation," EM 314-60, Jet Propuslion Laboratory, Pasadena, Calif., Aug. 24, 1976 (an internal document).

6. *NASA Directory of Observation Station Locations, 3rd Edition*, Goddard Space Flight Center, Vol. 1, Nov. 1973.

7. Marsh, J. G., Douglas, B. C., and Losko, S. M., "A Global Station Coordinate Solution Based Upon Camera and Laser Data - Goddard Space Flight Center 1973," Report X-592-73-177, Goddard Space Flight Center, May 1973.

8. Fanselow, J. L., et al., "Determination of UTI and Polar Motion by the Deep Space Network Using Very Long Baseline Interferometry," IAU Symposium 82, May 1978.

9. Campbell, J. K., and Rinker, G. C., "An Evaluation of Deep Space Network Station Locations from the Viking Encounters," EM 314-107, Jet Propulsion Laboratory, Pasadena, Calif., Jan. 11, 1977 (an internal document).

Table 1. Relative coordinate differences based on geodetic survey information

Station pair	Longitude, deg	Spin axis, km	Z-height, km
11-12[a]	−0.0439311	−5.71166	8.136
13-12[a]	0.0105998	3.43285	−4.672
14-12[a]	−0.084045	−8.05467	11.424
43-42	0.0	−0.10110	0.167
44-42	0.00347689	−11.37076	−16.765
62-61	−0.1188072	−1.79030	2.023
63-61	0.0010142	−0.15712	−0.226

[a]Survey based on DSS 12 before modification to 34-m antenna.

Table 2. VLBI results for intercontinental baseline

Station pair	Polar component, km
63-14	438.0561
32-14	−7351.8023
63-43	7789.8584

Table 3. Summary of radiometric data used in LS46 and LS47

	Tracking arc	Stations	Data types and number of measurements
Mariner IV encounter	7/6/65→7/28/65 (Enc: 7/15/65)	11, 42, 51	Doppler – 899
Mariner V pre-encounter zero declination arc	7/22/67→9/16/67	11, 12, 14 42, 61, 62	Doppler – 986
Mariner V encounter	10/14/67→10/25/67 (Enc: 10/19/67)	12, 14, 41, 62	Doppler – 759
Mariner V post-encounter zero declination arc	10/29/67→11/21/67	12, 14, 41, 62	Doppler – 704
Mariner VI encounter	7/25/69→7/31/69 (Enc: 7/31/69)	12, 14, 41 51, 62	Doppler – 642 Tau range – 322
Mariner IX encounter	11/9/71→11/13/71 (Enc: 11/14/71)	12, 14, 41, 62	Doppler – 798 Mu range – 6
Mariner X Venus encounter	1/28/74→2/14/74 (Enc: 2/5/74)	12, 14, 42 43, 62, 63	Doppler – 4162
Mariner X Mercury I encounter	3/21/74→4/10/74 (Enc: 3/29/74)	12, 14, 42 43, 62, 63	Doppler – 1871 Mu 2 range – 43 Plop range – 68
Viking I encounter	6/10/76→6/19/76 (Enc: 6/19/76)	11, 14, 43, 61, 63	Doppler – 641 Plop range – 43
Viking II encounter	7/28/76→8/7/76 (Enc: 8/7/76)	11, 14, 42, 43, 61	Doppler – 586 Plop range – 43

Table 4. Location set 45

Station	Spin axis, km	Longitude, deg	Z-height, km
11	5206.340046	243.1506103	3673.764
12	5212.051731	243.1945377	3665.628
13	5215.484580	243.2051375	3660.956
14	5203.996994	243.1104930	3677.052
41	5450.203099	136.8875110	-3302.189
42	5205.351556	148.9812947	-3674.588
43	5205.251036	148.9812975	-3674.755
44	5193.980796	148.9778178	-3691.353
51	5742.939395	27.6854493	-2768.744
61	4862.608228	355.7509964	4114.878
62	4860.818049	355.6321890	4116.901
63	4862.451240	355.7520093	4115.104

Table 5. Location set LS46

Station	Spin axis, km	Longitude, deg	Z-height, km
11	5206.339972	243.15061282	3673.764
12	5212.051635	243.19453947	3665.628
13	5212.484485	243.20513927	3660.956
14	5203.996942	243.11049354	3677.052
41	5450.203117	136.88751270	-3302.189
42	5205.351635	148.98129334	-3674.5833
43	5205.251074	148.98129542	-3674.7503
44	5193.980875	148.97781645	-3691.3483
51	5742.939341	27.68544919	-2768.744
61	4862.608297	355.75099792	4114.8821
62	4860.817979	355.63219164	4116.9051
63	4862.451306	355.75200886	4115.1081

Table 6. Analysis of LS46 spin axis and longitude update

Station	LS46/LS45	Effect of Viking data
	Spin radius, m	
11	-0.074	-0.006
12	-0.096	-0.015
14	-0.052	-0.040
41	0.018	0.010
42	0.079	0.060
43	0.038	0.063
51	-0.054	-0.007
61	0.068	0.046
62	-0.070	-0.024
63	0.066	0.019
	Longitude, 10^{-5} deg	
11	0.25	0.100
12	0.18	0.072
14	0.05	0.072
41	0.17	0.069
42	-0.14	-0.041
43	-0.33	-0.133
51	-0.01	-0.029
61	0.15	0.17
62	0.26	0.098
63	-0.04	-0.12

Table 7. Location set LS47

Station	Spin axis, km	Longitude, deg	Z-height, km
11	5206.339943	243.15060463	3673.764
12(34M)	5212.054081	243.19453139	3665.6298
12(26M)	5212.051599	243.19453139	3665.628
13	5215.484840	243.20513119	3660.956
14	5203.996900	243.11048519	3677.052
41	5450.203047	136.88750535	-3302.189
42	5205.351564	148.98128494	-3674.5833
43	5205.250988	148.98128679	-3674.7503
44	5193.980804	148.97780805	-3691.3483
51	5742.939219	27.68544265	-2768.744
61	4862.608263	355.75098948	4114.8821
62	4860.817963	355.63218340	4116.9051
63	4862.451243	355.75200027	4115.1081

Table 8. LS47/LS46 difference

Station	Spin axis, m	Longitude $\times 10^{-5}$ deg
11	-0.029	-0.819
12	-0.036	-0.808
14	-0.043	-0.835
41	-0.070	-0.735
42	-0.071	-0.840
43	-0.086	-0.863
44	-0.071	-0.840
51	-0.121	-0.654
61	-0.033	-0.844
62	-0.017	-0.825
63	-0.063	-0.856

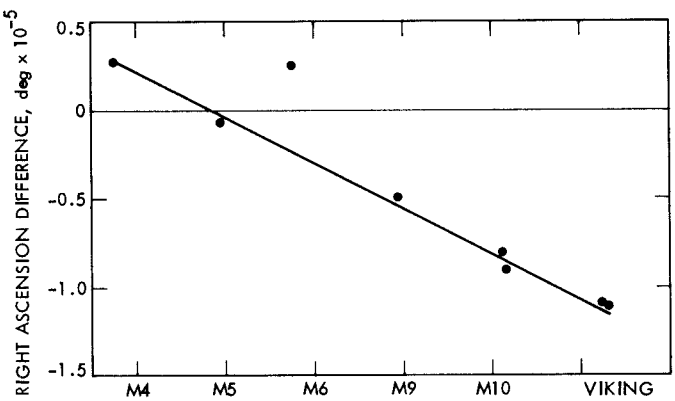

Fig. 1. DE108 and DE96 right ascension differences at planetary encounter

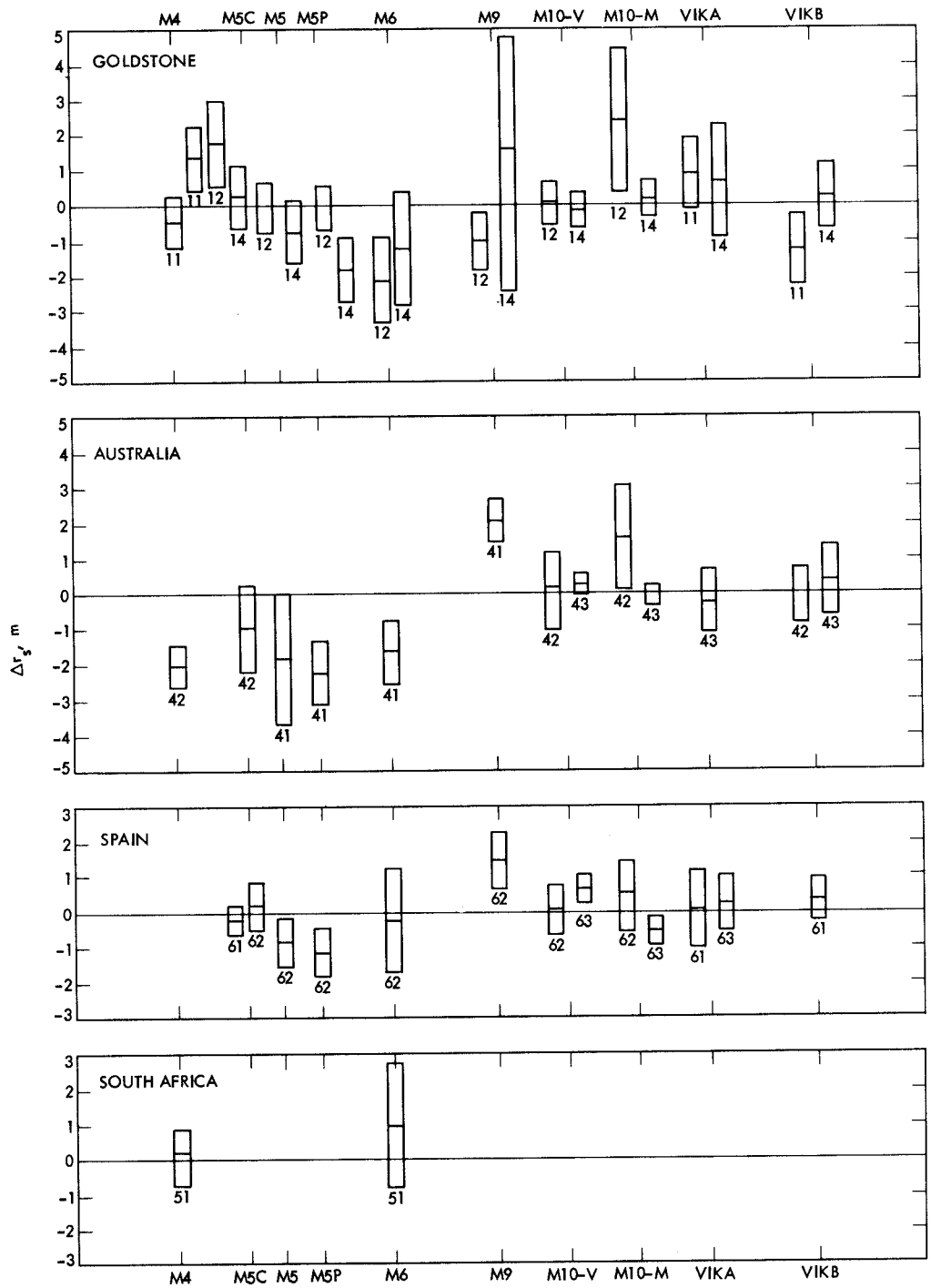

Fig. 2. Difference between individual data arc spin radius estimates and the DE96 solution, LS46

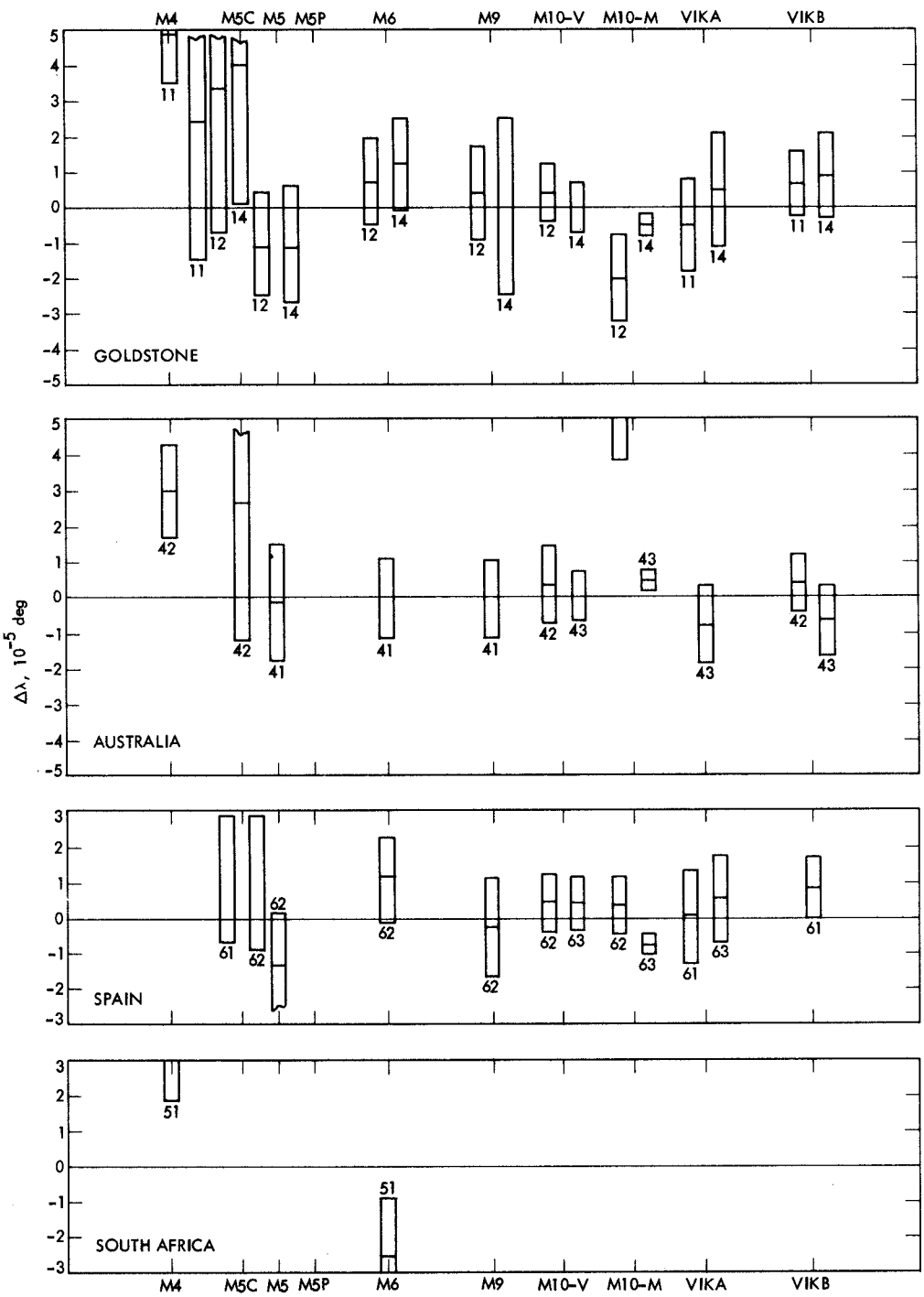

Fig. 3. Difference between individual data longitude estimates and the DE96 solution, LS46

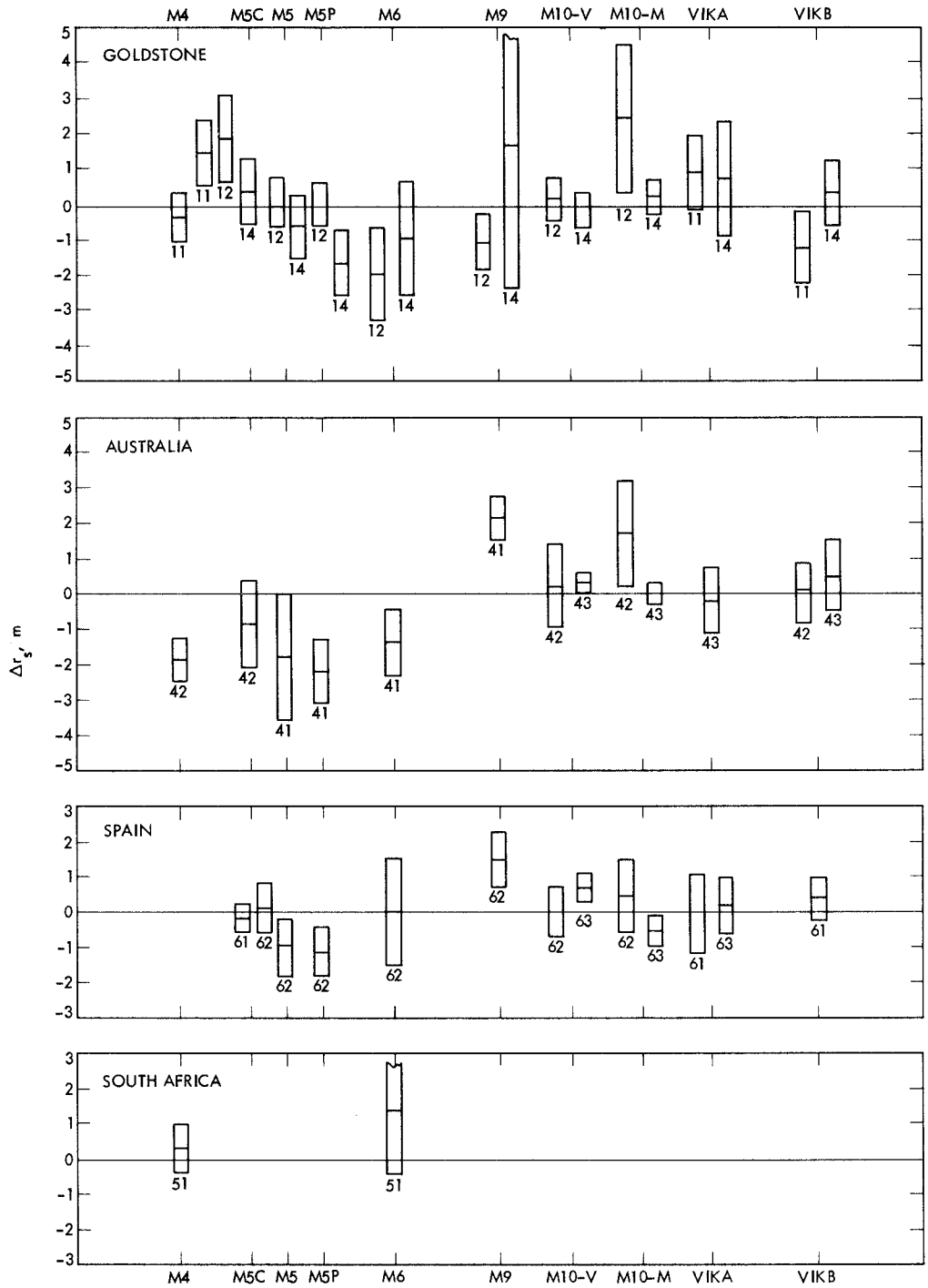

Fig. 4. Difference between individual data arc spin radius estimates and the DE108 solution, LS47

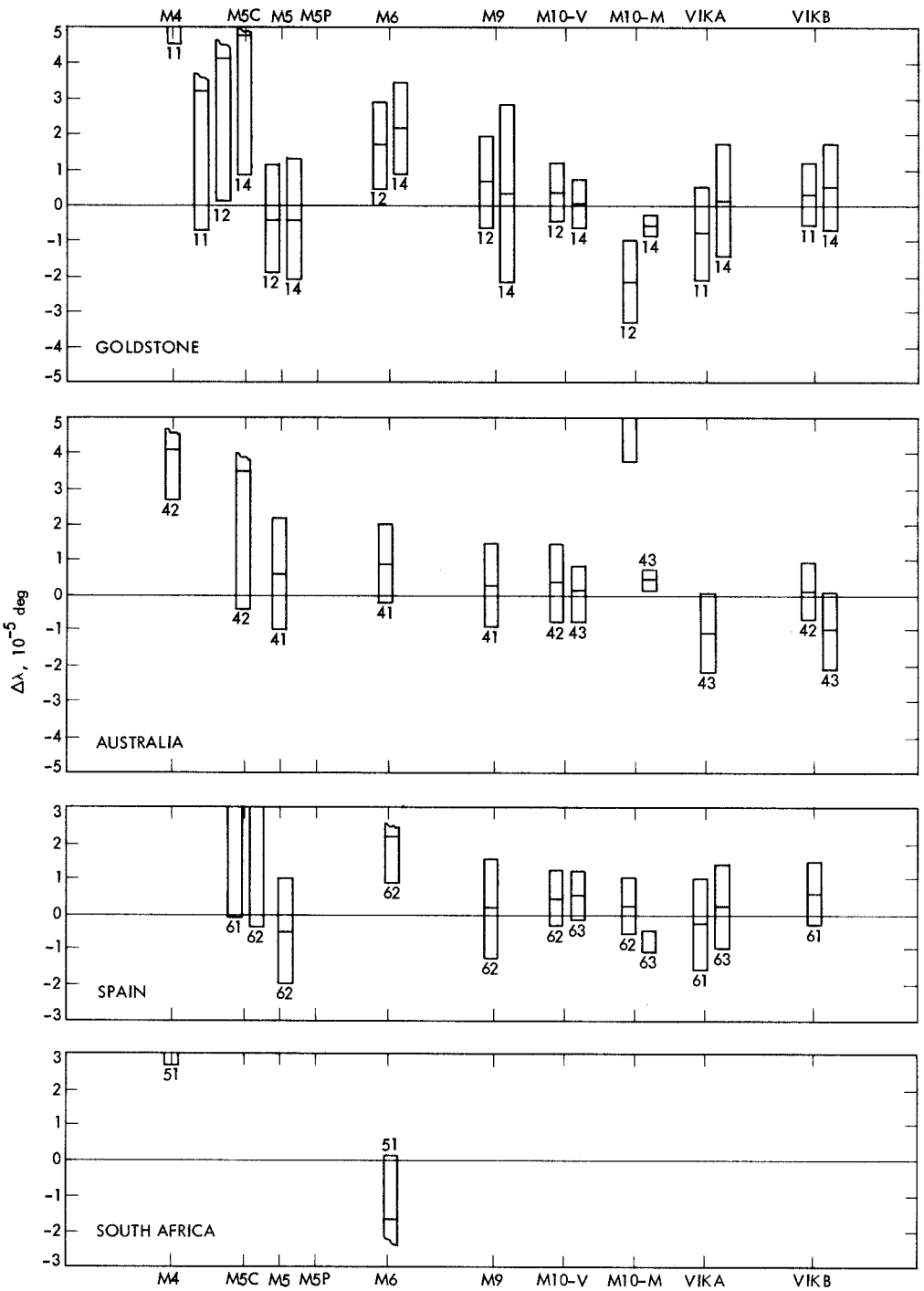

Fig. 5. Difference between individual data arc longitude estimates and the DE108 solution, LS47